Neuron, Volume *55*

Supplemental Data

Differential Attention-Dependent Response Modulation across Cell Classes in Macaque Visual Area V4

Jude F. Mitchell, Kristy A. Sundberg, and John H. Reynolds

Supplemental Results

Firing Rate Modulation During Object Tracking Across the Population as a Whole

To facilitate comparison with earlier single unit studies of attention, we analyzed attention-dependent changes in firing rate across the undifferentiated neural population. We recorded 218 neurons (142 in monkey A, 76 in monkey B), of which 160 were visually responsive (108 in monkey A, 52 in monkey B). Unless otherwise noted, all results were individually significant for each animal and did not differ significantly between animals. Supplemental Figure 1B shows the average firing rate of the visually responsive neurons to attended and unattended stimuli (dark grey-attended, grey-unattended). The response begins when the stimulus enters the receptive field, about 400 ms prior to the pause. We used the response during the pause period to analyze attention-dependent response changes. Unless stated, all statistical tests were non-parametric and two-tailed (Wilcoxon signed rank tests for paired observations, Mann-Whitney U tests for unpaired observations). Attended targets evoked a significantly stronger response compared to identical distracters (mean attended = 19.4 Hz, mean unattended = 16.5 Hz, paired, $p<0.001$). We also examined the percentage increase in the response above baseline to attended stimuli over the response to unattended stimuli. McAdams and Maunsell (1999a, 1999b) found a median percentage increase of 26% in the response with baseline subtracted for area V4 neurons in a standard match-to-sample attention paradigm. We find a comparable median increase of 22.9%.

We computed attention indices as described in the main text. The attention index, AI=(A-U)/(A+U), provides a measure of the proportional change in response that is unbiased in that its expected value is zero if there is no attention effect. Another commonly used measure, the ratio A/U, gives a distribution that is skewed to the right even for identical random distributions of A and U. Although this does not bias the estimate of the median, nor alter the results for non-parametric tests based on medians, it is biased in the mean.

The distribution of attention indices for the firing rate across the whole population is shown in Supplemental Figure 1C. Attention indices were shifted to the right of zero, indicating increased responses with attention (paired, $p<0.001$). Of 160 neurons, 79, indicated in black, showed significant attention-dependent changes in firing rate (paired test for a difference in mean rate on attended versus unattended trials, $p<0.05$). Of these, 68 showed significant attention-dependent increases in firing rate and 11 showed significant decreases.

Attention-dependent Changes in Response Variability Across the Population as a Whole

The Fano factor, the ratio of spike count variance to mean spike count, provides a measure of response variability. To examine whether response variability changed with attention, we computed the Fano factor for each neuron, and compared this measure across attention conditions. Supplemental Figure 1D shows the Fano factor computed over successive 100 ms bins and then averaged across all visually responsive neurons for attended and unattended stimuli, shown in dark grey and grey, respectively. Fano factors computed on responses evoked by attended targets were significantly reduced compared to identical distracters (mean attended = 1.31, mean unattended = 1.48, paired $p<0.001$). We also examined modulation in variability in terms of the percentage change of the unattended Fano factor. There was a median decrease of 10.1%, which was statistically significant (paired, $p<0.001$). To assess the distribution of changes, we computed a Fano factor modulation index for each neuron, defined as (A-U)/(A+U) where A is the mean Fano factor for attended stimuli and U is the mean Fano factor for identical unattended stimuli. The distribution of indices appears in Supplemental Figure 1E. The distribution was significantly shifted to the left of zero, corresponding to a reduction in Fano factor (paired, $p <0.001$). Of the 160 neurons recorded from both animals, 38, indicated in black, showed significant changes in Fano factor (Monte-Carlo sampling, $p<0.05$, see main text Methods). Of these, 36 showed significant reductions in Fano factor while only 2 showed significant increases.

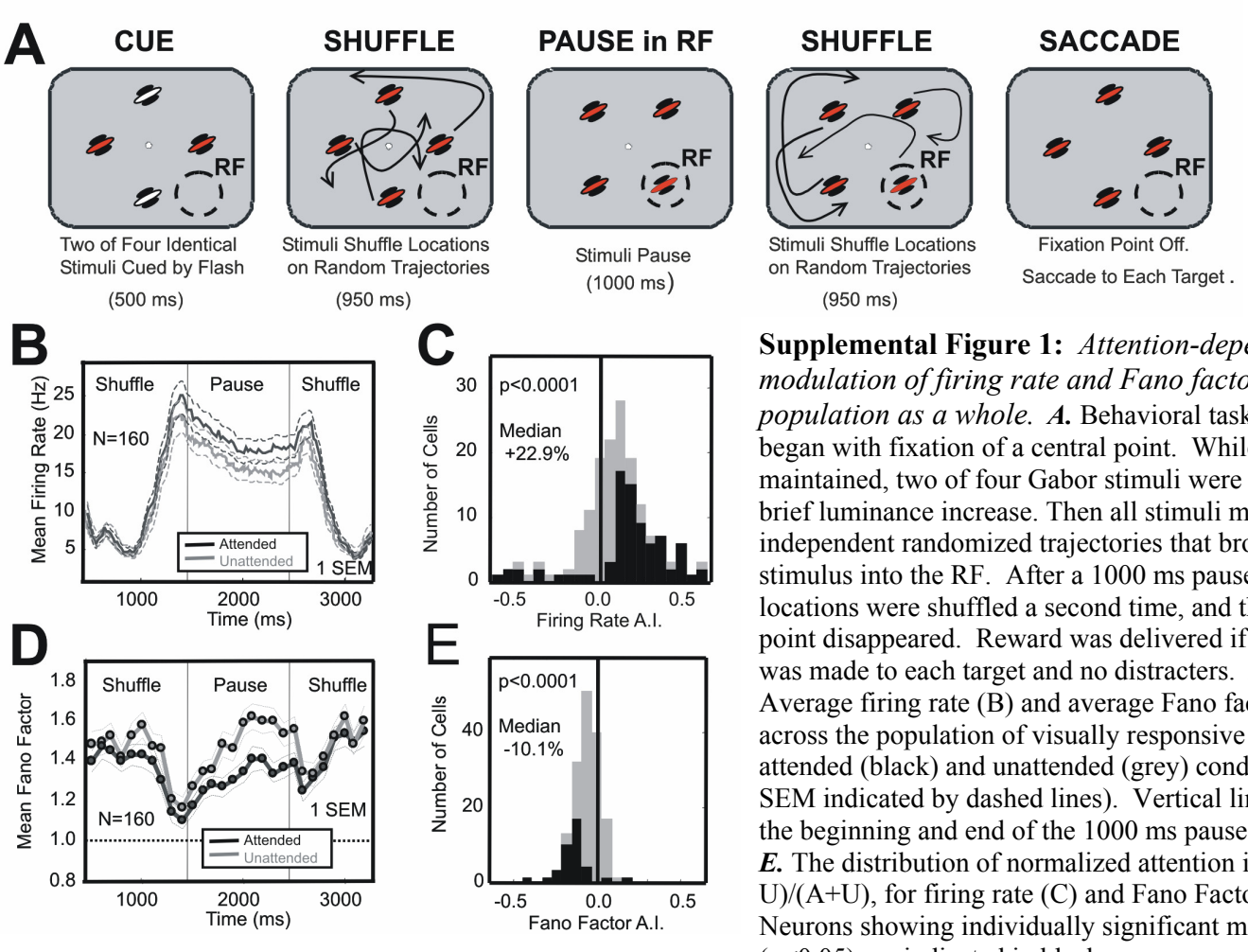

Supplemental Figure 1: *Attention-dependent modulation of firing rate and Fano factor across the population as a whole.* ***A.*** Behavioral task. Each trial began with fixation of a central point. While fixation was maintained, two of four Gabor stimuli were cued with a brief luminance increase. Then all stimuli moved along independent randomized trajectories that brought one stimulus into the RF. After a 1000 ms pause, stimulus locations were shuffled a second time, and the fixation point disappeared. Reward was delivered if a saccade was made to each target and no distracters. ***B, D.*** Average firing rate (B) and average Fano factor (D) across the population of visually responsive neurons for attended (black) and unattended (grey) conditions (+/- 1 SEM indicated by dashed lines). Vertical lines indicate the beginning and end of the 1000 ms pause period. ***C, E.*** The distribution of normalized attention indices, (A-U)/(A+U), for firing rate (C) and Fano Factor (E). Neurons showing individually significant modulation ($p<0.05$) are indicated in black.

Does isolating single units based on PCA clustering of waveforms artificially contribute to bimodal distributions in waveform duration?

One might imagine that our methods for isolating single units could have favored selection of units with distinguishable waveforms and thus biased our sample towards a bimodal distribution. Our V4 sample included only units that had been clearly isolated based upon clustering in the principle components of the waveforms on each electrode (Offline Sorter, Plexon, Inc.). It is often possible to isolate two or more units on the same electrode using clustering when their waveforms differ substantially. For example, the two units depicted in Supplemental Figure 2A were recorded on the same electrode but could be clearly separated based on differences in their waveform shape. If our analysis included such distinguishable pairs, but excluded others in which waveforms were paired with more intermediate shapes, then we could be biased to observe a bimodal distribution artificially.

To test whether our isolation methods contributed to the bimodality observed, we examined the waveforms in area V4 from this and one other ongoing experiment (N=287 total units) and isolated the subset of recordings where only one action potential was isolated per electrode (N=115 units). The distribution of waveform durations from this subset, shown in dark green in Supplemental Figure 2B, remains significantly bimodal according to Hartigan's Dip test (p=0.0047) (Hartigan and Hartigan, 1985; Mechler and Ringach, 2002). Thus the bimodal distribution observed is not an artifact of our algorithm for distinguishing between simultaneously recorded action potentials.

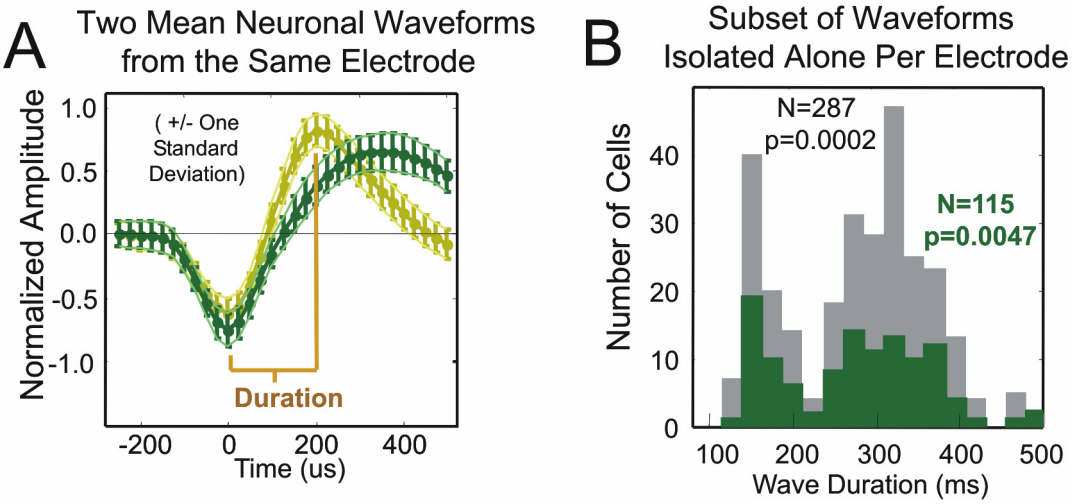

Supplemental Figure 2: *Single unit isolation through waveform clustering does not account for the bimodality in waveform duration.* ***A.*** The mean waveforms (+/- one standard deviation) of two neurons recorded from the same electrode. Though recorded on the same electrode, action potentials from these units could be clearly separated based upon the their shape and duration. Waveform duration was defined as the time, in microseconds, from waveform trough to peak. ***B.*** A larger distribution of waveform durations collected from the current and one other ongoing experiment is shown here in grey. Superimposed in dark green is the distribution from the subset of recordings where a single action potential was isolated per electrode. The distribution is significantly bimodal (Hartigan's Dip test, p=0.0047), indicating that the bimodality is not an artifact of isolating distinguishable waveforms.

The distribution of firing rate, Fano Factor, and their modulation by attention as a function of waveform duration.

In the main text the distribution of attention modulation effects across the population are summarized by histograms of the attention indices for narrow spiking (duration <= 200 μs) and broad spiking (duration > 200 μs) neurons. These histograms are highly compressed descriptions of the data. To provide an indication of variance in the data, these indices and other response measures are plotted against spike duration in Supplemental Figure 3. Supplemental Figure 3A shows the firing rate for an unattended stimulus (y-axis) versus waveform duration (x-axis), for each visually responsive neuron that could be categorized as narrow or broad spiking on the basis of its waveform (N=152). Supplemental Figures 3B, 3C and 3D show, respectively, Fano Factors for unattended stimuli, firing rate A.I. indices, and Fano factor A.I. indices, plotted as a function of waveform width. Firing rate A.I.'s (Supplemental Figure 3C) are more variable for longer duration action potentials, but indices mainly fall above zero for both classes, indicating a tendency to increase firing rate with attention. The percentage modulation of the Fano Factor (Supplemental Figure 3D) is significantly negative for both classes, indicating a decrease in spiking variability with attention, with greater modulation among those neurons with shorter duration waveforms.

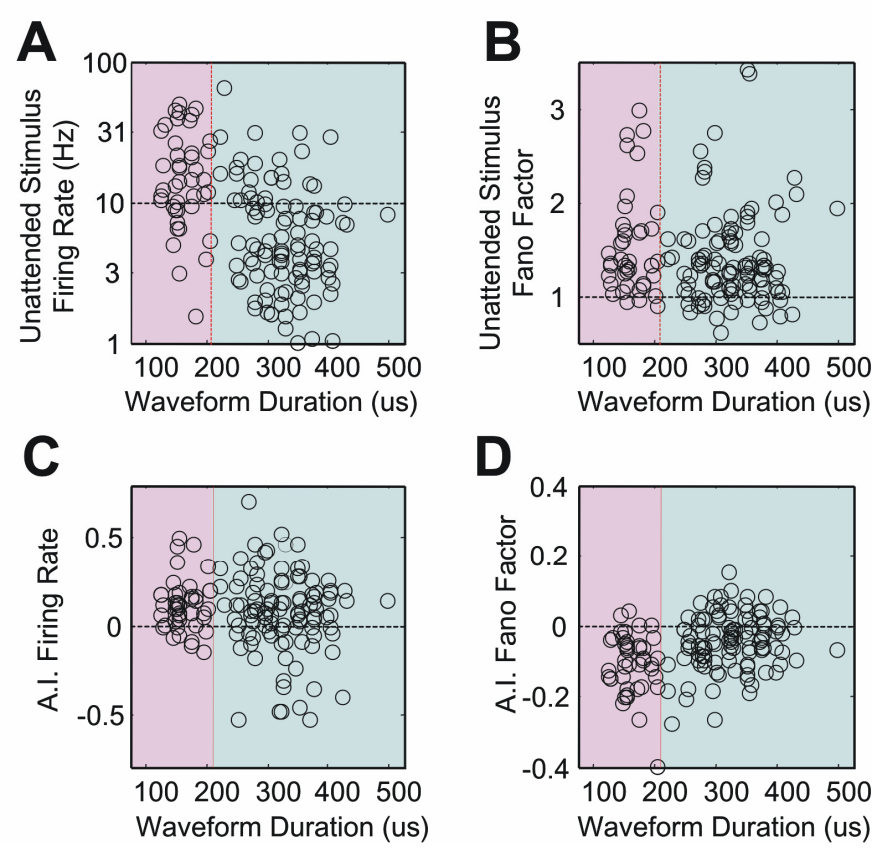

Supplemental Figure 3: *Scatter plots of firing rate,Fano Factor, AI indices of firing rate, and AI indices of Fano Factor against waveform duration.* ***A.*** The mean firing rate during the pause period to an unattended stimulus plotted against the waveform duration. Each point corresponds to a visually responsive neuron that had a well-defined waveform duration (N=152). ***B.*** The mean Fano Factor during the pause period to an unattended stimulus plotted against the waveform duration for each unit. ***C.*** The attention modulation index (A.I. index) of firing rate plotted against the waveform duration. ***D.*** The A.I. index of Fano Factor plotted against the waveform duration.

Differences in mean firing rate between broad and narrow spiking classes do not explain the difference in Fano Factor reduction between classes

As an additional test of whether the stronger attention-dependent reduction in Fano Factor among narrow spiking neurons was due to their higher firing rates, we performed an analysis that equated the firing rates of individual neurons across attention conditions. For each neuron we obtained 10 rate-variance pairs in each attention condition computed from the ten 100 ms bins during the pause period. We then identified the subset of pairs that could be matched in mean firing rate across attention conditions, as illustrated for an example neuron in Supplemental Figure 4A. Red lines connect samples from attended and unattended conditions in which the mean spike count (horizontal axis) was within 5%. The spike count variance for each pair is indicated on the vertical axis. We then computed the mean Fano factor averaged across these rate-matched pairs. To confirm that this rate matching procedure eliminated differences in mean firing rate, we examined the distribution of firing rate attention indices before and after this procedure for narrow and broad spiking classes (Supplemental Figure 4B, lower panels labeled "Rate Matched"). As intended, after rate matching there were no longer any significant differences in firing rate between attention conditions, as indicated by attention indices clustering at zero. Supplemental Figure 4C shows the distribution of Fano Factor attention indices for broad spiking neurons (top panels) and narrow spiking neurons (bottom panels) before and after rate matching. The attention-dependent reduction in Fano factor remained significant among the narrow spiking neurons after rate matching (median 9.2% reduction, Wilcoxon signed rand test, $p<0.001$) indicating that it was not due to changes in firing rate. The reduction after rate matching was no longer significant for broad spiking neurons (Wilcoxon signed rank test, $p=0.082$), suggesting that it may be due to changes in the firing rate combined with saturation in variance due to a relative refractory period. This is consistent with the analyses illustrated in Figure 3 of the main text. The attention-dependent Fano factor reduction among narrow spiking neurons remained significantly stronger than that of broad spiking neurons (Mann Whitney U test, $p=0.0174$). In short, the difference in attention-dependent Fano factor modulation reflects a genuine difference between classes that is not due to their different firing rates.

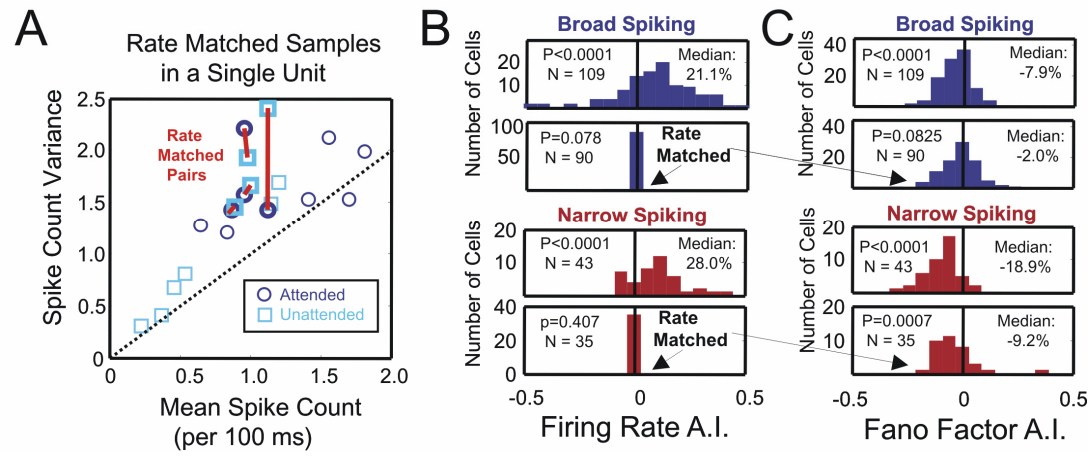

Supplemental Figure 4: *Attention-dependent modulation of spiking variability in broad and narrow spiking neurons after rate matching individual neurons.* (Caption next page).

Supplemental Figure 4 (Caption): *Attention-dependent modulation of spiking variability in broad and narrow spiking neurons after rate matching individual neurons.* ***A.*** For each individual neuron, we compared the ten samples of spike rate and variance from each of the ten 100 ms bins within the pause period, for attended and unattended conditions. In random order we searched each unattended rate-variance pair to identify a match to an attended rate-variance pair that differed by no more than 5% in firing rate. Red lines illustrate examples of matched pairs for one example neuron. If three or more pairs could be rate-matched, the neuron was included for further analysis. The Fano factor was then computed from the mean variance and mean spike count for each of these rate-matched neurons. ***B.*** First and third panels: distribution of attention indices before rate matching. Second and fourth panels: After rate matching, there was, as a result of the rate matching procedure, no longer a significant difference in firing rate across attention conditions. ***C.*** The distribution of Fano factor attention indices before and after controlling for differences in firing rate across the two populations. The indices remain significantly shifted to the left (indicating a reduction in variability) among narrow spiking neurons, after equating firing rates within each cell. The reduction in Fano factor among broad spiking neurons was no longer significant after controlling for firing rate. The narrow spiking neurons still show stronger reductions in Fano factor than broad spiking neurons (Mann-Whitney U test, $p = 0.0174$) after controlling for rate.

Eye position analysis

We tested whether shifts in eye position could have contributed substantially to the attention-dependent modulations in firing rate. Both monkeys had a small but significant shift in position away from the RF when the stimulus in the RF was attended (Supplemental Figure 5A and Figure 5B). The position offsets were small (Monkey A, mean 0.03 degrees, Wicoxon signed rank test $p<0.01$; Monkey B, mean 0.08 degrees, Wicoxon signed rank test $p<0.01$) relative to the size of the receptive fields, which were at least 3 degrees in diameter (median RF eccentricity was 7.5 degrees). If the attention-dependent firing rate modulation reflected shifts in eye position, then rate should increase with the deviation away from the RF. We therefore examined how the firing rate varied as a function of the shift in eye position for attended (red) and unattended (blue) trials (Supplemental Figure 5C and 5D). The change in rate with eye position did not increase systematically with the deviation of the eye away from the RF. Neuronal firing rates in both monkeys were higher for attended trials at matched eye positions. Further, few neurons individually showed significant correlations between rate and eye position (13 of 108 units in Monkey A, 6 of 52 units in Monkey B; $p<0.05$) and the slope of the best linear fit was not significantly different from zero across the population (Wilcoxon signed rank test; in Monkey A, median 1.9% decrease per degree away from RF, $p = 0.258$, in Monkey B, median 5.5% increase per degree away from RF, $p=0.082$). Thus, slight deviations in eye position do not account for the observed attention-dependent changes in firing rate.

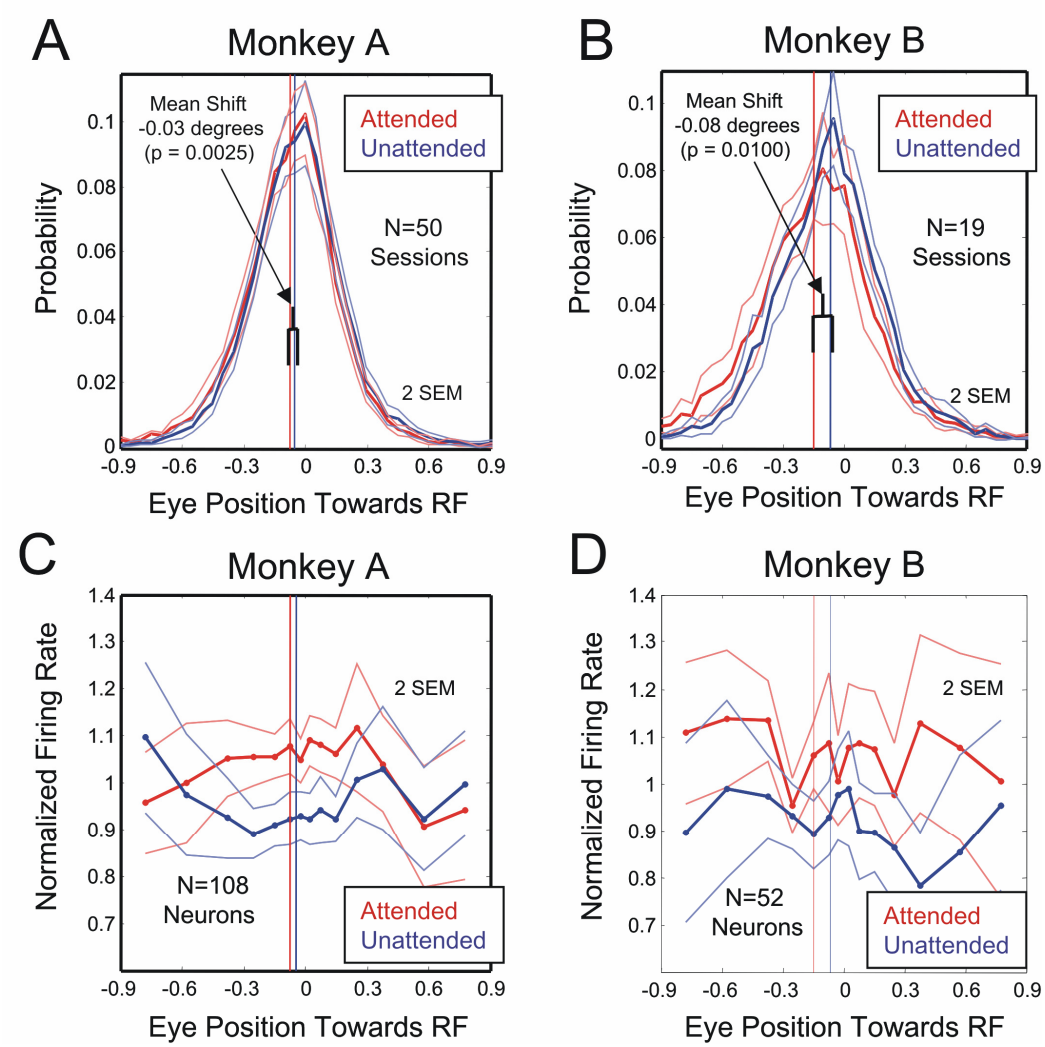

Supplemental Figure 5: *Attention-dependent shifts in eye position and the correlation of firing rate with eye position.* ***A,B***: The distribution of eye position, projected on the line passing through the center of the RF and the fixation point, computed during the pause period, for Monkey A and Monkey B. Red lines correspond to trials when the stimulus in the RF was attended, and blue when not attended. To correct for gradual shifts in the eye position over the recording session that were due to postural changes of the monkey (which can slightly shift the head position) we first subtracted off the mean eye position during the first 100 ms of each trial after fixation was acquired. This is prior to onset of the tracking stimuli. To generate the distributions shown, eye position was averaged for each 100 ms interval during the 1000 ms pause period when the stimulus was inside the RF, giving 10 samples per trial. No interval including a fixational eye movement was included in the analysis. Distributions were computed from 50 recording sessions in Monkey A and from 19 recording sessions in Monkey B. In both monkeys there was a small but significant shift in eye position away from the RF when the stimulus in the RF was attended, as indicated by a slight relative leftward shift in the peak of the distribution derived from trials when attention was directed to the stimulus in the RF. ***C,D***: The average normalized firing rate as a function of the eye position, is shown for Monkey A and Monkey B respectively. We computed the spike count for each visually responsive neuron in each 100ms bin of the 1000 ms pause and the corresponding average eye position (10 sample pairs per trial). The spike counts were then averaged in bins along the eye position axis stepping from -0.8 to 0.8 degrees. Responses were then normalized by the mean spike count averaged from both attention conditions. In both monkeys the changes in rate with eye position were modest, even over a range of positions that was far larger than the slight deviation in mean eye position across cueing conditions. Firing rate at matched eye positions was higher for attended stimuli.

Eye drift analysis

Slow changes in the drift of the eyes could also potentially influence V4 responses. We thus measured eye velocity as a function of attention condition. Monkey A showed no significant changes in eye velocity between attention conditions (Supplemental Figure 6A) while Monkey B had a small but significant drift away from the RF when the stimulus in the RF was attended (Supplemental Figure 6B). The change in velocity was small in both monkeys (Monkey A, mean 0.01 degrees/s, Wicoxon signed rank test $p=0.31$; Monkey B, mean 0.06 degrees/s, Wicoxon signed rank test $p<0.05$), so it is unlikely that it contributed to the observed effects. To examine this more closely, we quantified firing rate varied as a function of the eye velocity for attended (red) and unattended (blue) trials (Supplemental Figure 6C and 6D). As was the case for eye position, the change in firing rate does not increase systematically with the eye velocity away from the RF. Further, neuronal firing rates in both monkeys were higher for attended trials at matched eye velocity.

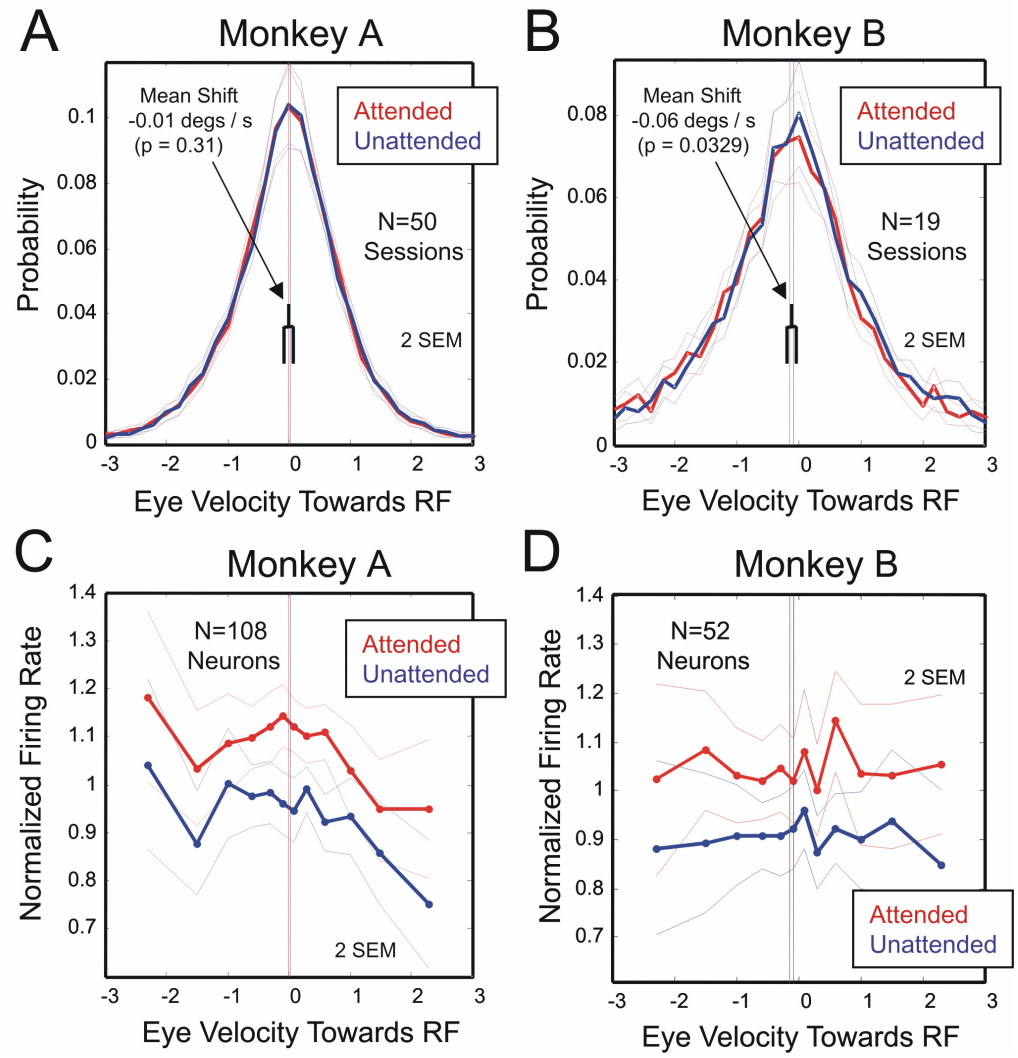

Supplemental Figure 6: *Attention-dependent changes in eye velocity and the correlation of firing rate with eye velocity.* ***A,B***: The distribution of eye velocity, projected on the line passing through the center of the RF and the fixation point, computed during the pause period, for Monkey A and Monkey B. Red lines correspond to trials when the stimulus in the RF was attended, and blue when not attended. Data were generated as in Supplemental Figure 5, but using the eye velocity in place of eye position. Monkey A had no significant change in eye velocity. Monkey B had a modest drift away from the RF when the stimulus in the RF was attended, as indicated by a leftward shift in the attended (red) distribution. ***C,D***: The average normalized firing rate as a function of the eye velocity, for Monkey A and Monkey B respectively. The changes in rate with eye velocity were modest. Firing rate at matched eye velocities was higher for attended stimuli.

Fixational eye movement analysis

An important consideration is the role that small fixational eye movements might have played in the reduction in spiking variability that was observed with attention. Previous studies have shown that variability in firing rate among neurons in primary visual cortex is reduced when intervals containing fixational movements are eliminated from analysis (Gur et. al., 1997; Gur and Snodderly, 2006). Fixational movements can cause strong transients in firing among neurons in primary visual cortex (Martinez-Conde et. al., 2000) as well as other extra-striate areas, including area V4 (Leopold and Logothetis, 1998). If the frequency, direction, or amplitude of fixational eye movements varied between attention conditions, they might produce the observed reduction in variability. A priori, this seems an unlikely possibility because during all trials the monkeys maintained attention on two of the four peripheral targets. Thus there is no particular reason to believe that the eye movements would differ depending on whether or not a target was inside the receptive field.

To test this directly we measured fixational eye movements across attention conditions, and examined whether they modulated the response of V4 neurons in our population. Although the infarared eye trackers used in this experiment do not give as precise an estimate of eye position as scleral coils they do provide enough precision to identify fixational eye movements. Eye data for Monkey A was recorded at higher spatial resolution (mean discretization of 0.07 degrees) than Monkey B (discretization of 0.20 degrees, reflecting differences in ISCAN parameters). We therefore focused our fixational eye movement analysis on Monkey A where we could test the possible effects of smaller movements. Two example eye traces for Monkey A are shown in Supplemental Figure 7A and 7B with identified saccade events (indicated by red vertical lines). Details of the saccade detection algorithm are outlined in the figure caption. The source code with example data is provided at http://www.snl.salk.edu/~jude/. Eye movements as small as 0.1 degrees of visual arc could be successfully identified in Monkey A.

We confirmed the effectiveness of our saccade detection by examining the metrics of the identified saccades. Previous studies have demonstrated that a nearly linear relation between saccade amplitude and peak movement velocity that is observed for larger saccades (Zuber et. al., 1965), persists even among fixational eye movements (Bair and O'Keefe, 1998; Martinez-Conde et al, 2000). A similar relationship can be seen for the saccades detected in Monkey A (Supplemental Figure 7C, black dots) when compared to the linear fit reported in previous studies (blue line). There were, on average, 1.09 fixational saccades per second, the mean saccade amplitude was 0.30 degrees, and the mean saccade duration was 34.8 +/- 8.4 ms.

We considered whether fixational movements caused a significant modulation of the firing rate among the V4 neurons in our population (Supplemental Figure 7D). For both attended (shown in red) and unattended (blue) trials, there was a transient dip in firing rate 50-150 ms after saccade onset followed by an increase at 150-300 ms after onset. The average percentage decrease in firing from 50 to 150 ms relative to that of the rate in the 200 ms preceding saccade onset was 11.7% ($p<0.001$, Wilcoxon signed rank

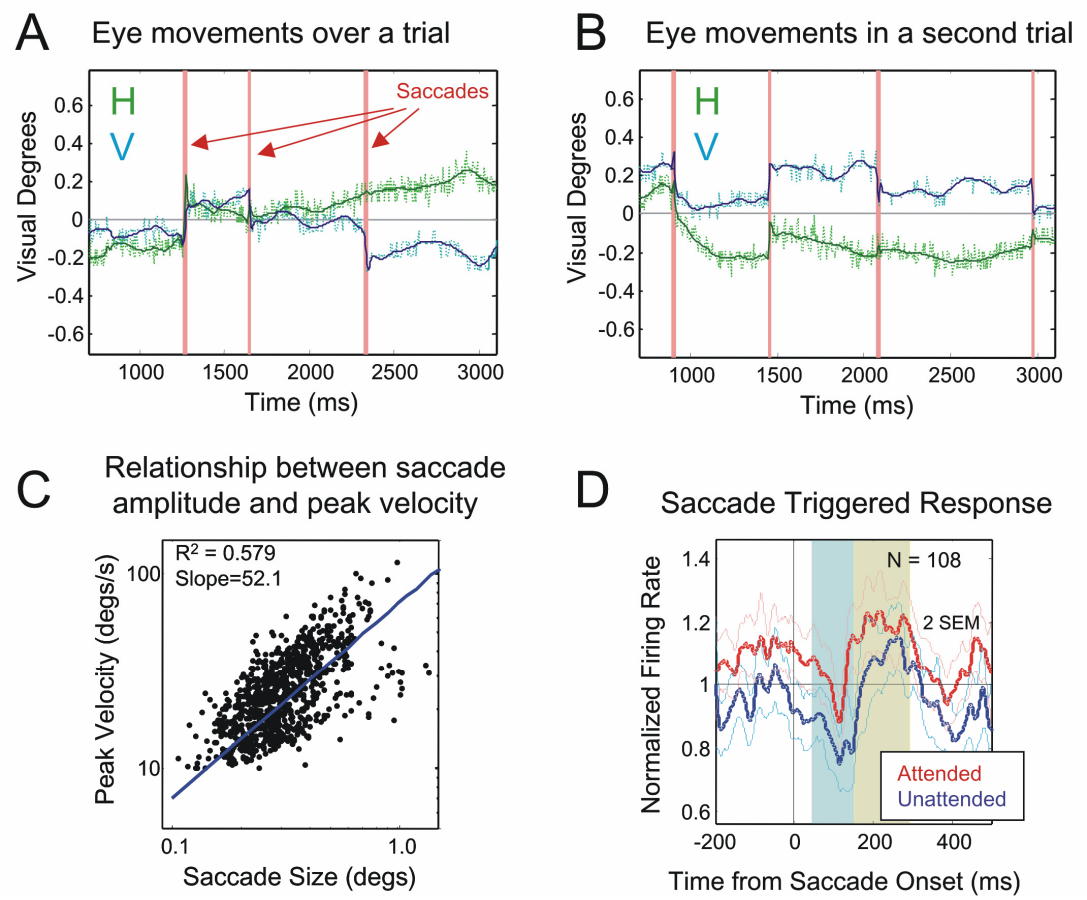

Supplemental Figure 7: *Fixational eye movements and their modulation of V4 neuronal firing.* ***A,B:*** Horizontal eye position (green dashed line) and vertical eye position (blue dashed line) is shown over two typical trials. The saccade detection algorithm tests each time point in the horizontal and vertical position traces over a trial to determine if in a 400 ms window surrounding that time point the position traces are better fit using a model that includes a saccade-like discontinuity at that point compared to a smooth polynomial spline function with an equal number of free parameters. The discontinuity model included a low order spline with mean, linear, and quadratic terms plus a sigmoid step function at the center of the 400 ms interval that had width and amplitude parameters and two other amplitude parameters for the 1st and 2nd derivatives of that sigmoid (7 parameters total). Model parameters were determined by minimizing the mean squared error. The model fit to the position traces is shown in dark green and dark blue. Those points at which the variance explained by the discontinuity model was more than 30% over the spline, that exceeded a 10 deg/s velocity threshold, and that exceeded a 1000 deg/s^2 acceleration threshold were identified as saccades (indicated by red vertical lines). ***C:*** A linear relationship between saccade amplitude and the peak velocity of fixational eye movements is observed. Saccade amplitude was measured as the maximum change in position over the duration of the movement, with saccade onset and offset defined as the first and last milliseconds that the absolute value of acceleration crossed a threshold of 1000 deg/s^2. The linear trend was similar to that reported from human psychophysics shown by the blue line (velocity = 70 * saccade amplitude, Zuber et. al., 1965) and a previous study in the macaque (Bair and O'Keefe, 1998). ***D:*** The normalized firing rate time-locked to the onset of those fixational eye movements that occurred during the 1000 ms pause period when the stimulus in the RF was attended (red) or unattended (blue). Firing rate was normalized individually for each unit by the mean firing rate of the saccade triggered average computed from a null distribution in which trial identities (mixing both attended and unattended trials) were randomly shuffled and a saccade triggered average computed for each shuffle, with the result averaged from one thousand different shuffles.

test). The average percentage increase in firing rate from 150 to 300 ms relative to that of the rate in the 200 ms preceding saccade onset was 9.7% ($p<0.001$, Wilcoxon signed rank test). This fixational eye-movement-triggered change in firing rate validates our ability to detect fixational eye movements. Further, the fact that firing rate was elevated for attended trials throughout the time surrounding fixational eye movements demonstrates the attention-dependent increase in firing was not caused by the eye movements. It should be noted that the modulation in firing rate due to fixational movements is smaller than that reported in a previous study of V4 (Logothetis and Leopold, 1998). However, the previous study recorded from neurons with foveal receptive fields, where fixational eye movements are a larger fraction of the receptive field diameter, and used square-wave stimuli with hard edges. Either of these factors may explain the larger modulation observed in the earlier study.

Having validated our ability to detect fixational eye movements, we tested whether they differed across cueing conditions. There were no significant differences in the number, direction, or amplitude of fixational saccades during the 1000 ms pause period when the unattended or attended stimuli were positioned within the receptive field. As a final control analysis, we repeated the earlier analyses of rate and Fano factor for both narrow and broad spiking neurons after excluding all 100 ms intervals that followed within 400 ms after the onset of a fixational saccade. Excluding these intervals caused no significant changes in the results. In short no systematic differences in eye movements appear to contribute to the differences in firing variability with attention or to the differences in attention modulation between the narrow and broad spiking neuronal classes.

Burst firing in narrow and broad spiking neurons

Burst firing was evident among many neurons, as indicated by an excess of short duration (<5ms) inter-spike intervals (ISIs), relative to what would be expected from a Poisson process. Neurons with frequent burst events thus exhibit early peaks in their ISI distribution. The ISI distributions for two example neurons from our population appear in Supplemental Figure 8A and 8B. We used the response during the last 500ms of the pause period in the tracking task, during which the mean firing rate is relatively constant, in order to compute the distributions. The first neuron (Supplemental Figure 8A) has a largely exponential decay in its ISI distribution that is consistent with a Poisson process, and at the shortest ISIs has a dip that is due to the spike refractory period. By contrast, the second example unit (Supplemental Figure 8B) exhibits a sharp peak early in the ISI distribution at 2-3ms that is indicative of burst firing.

In order to better distinguish between regular and burst firing we fit two alternative parametric models to each ISI distribution. The first model is a simple Poisson process that includes spike refractory period (Supplemental Figure 8D). The spike refractory period is modeled as a brief Gaussian distributed delay that is equivalent to a previous study that used a Gaussian recovery function (Berry and Meister, 1998).

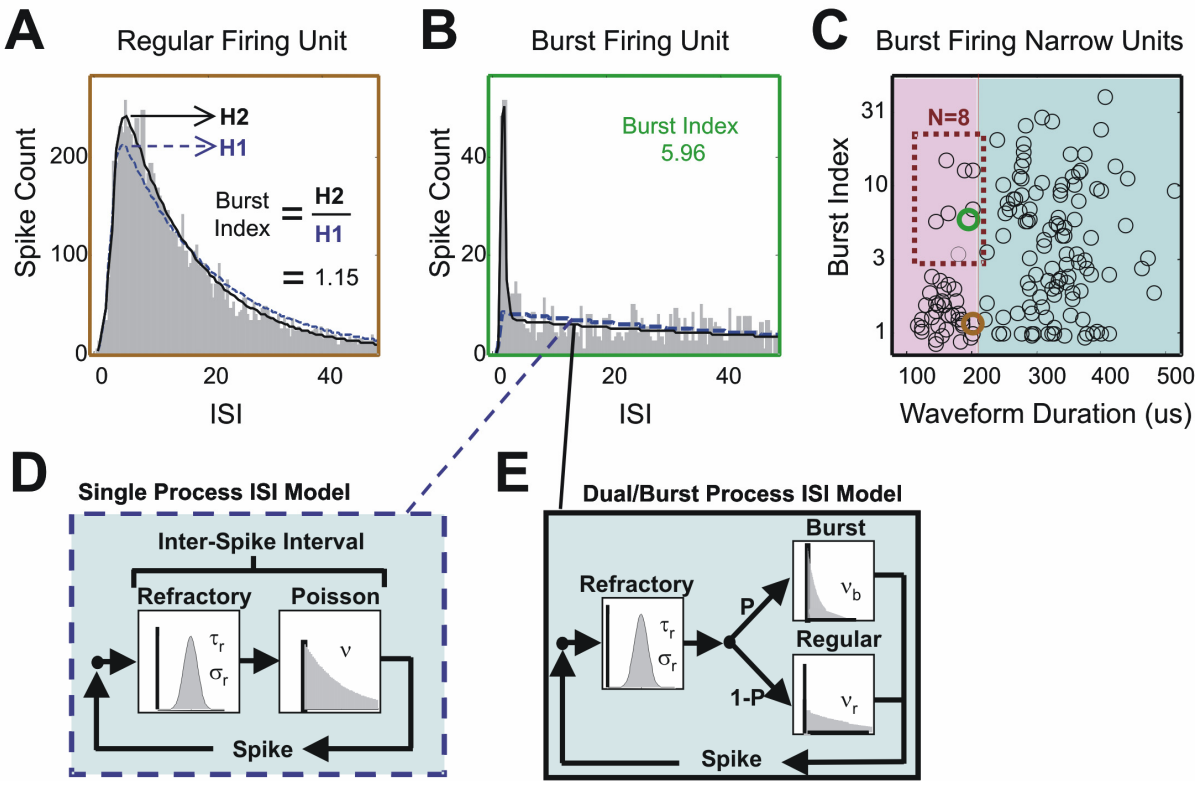

Supplemental Figure 8: *Inter-spike interval (ISI) distributions and evidence of burst firing in narrow spiking and broad spiking neurons.* ***A***: The distribution of inter-spike intervals in the first 50 ms (in increments of 0.5ms) for a regular firing unit. The blue dashed line indicates the single process fit (Poisson process with a spike refractory period) and the black line indicates the dual 'burst' process fit. The burst index for each unit was defined as the ratio of the height of the peak of the burst model fit (indicated by H2 in Panel A) relative to that of the single process fit (indicated by H1 in Panel B). The ISI distribution for this unit is relatively well fit by the single process fit. **B:** The ISI distribution of a second unit showing strong indications of burst firing. Spikes cluster at short intervals (<5ms) producing an early peak in the ISI distribution that cannot be adequately fit by the single process model (blue dashed line) and instead requires a burst model (black line). ***C***: The burst indices plotted against waveform duration for visually responsive units that could be identified as narrow or broad spiking on the basis of their waveform (N=152). Green and brown labeled points indicate the example units shown in Panels A and B. **D:** The inter-spike intervals of the single process model are generated by summing a Gaussian distributed random delay, which models the refractory period, and an exponentially distributed random variable, that models a Poisson process. **E:** The inter-spike intervals of the 'burst' process model includes an additional exponentially distributed random variable which is drawn from with probability P and has a higher firing rate that fits the firing rate during burst events.

This model can fit the initial dip in the ISI distribution that is due to the refractory period and the subsequent exponential decay, as can be seen for the first example unit (blue dashed line in Panel 8A). However, it cannot fit an early peak that is due to burst firing events, as can be seen in the second example unit (blue dashed line in Panel 8B). The second model is identical to the first model except that it draws probabilistically from two Poisson processes: one process that has a high rate consistent with the instantaneous rate that occurs during burst events (Supplemental Figure 8E), and a second process that has a low rate, consistent with the instantaneous rate that occurs during inter-burst intervals. This dual processes model provides a fit that is similar to the single process model when no early peak is present in the ISI distribution (black line in Panel 8A), but is capable of fitting early peaks when present, as can be seen for the second unit (black line in Panel 8B). Model parameters were fit by minimizing the Kullback-Leibler distance of the actual ISI distribution and the theoretical distribution. Matlab code to perform the fits, along with sample data, is available at http://www.snl.salk.edu/~jude/.

To quantify the burstiness of firing we computed a burst index defined as the ratio of the height of the peak of the burst model fit (indicated by H2 in Panel A) relative to that of the single process fit (indicated by H1 in Panel B). Supplemental Figure 8C shows this burst index plotted as a function of waveform duration, for all visually responsive units. Narrow spiking neurons tended to be less bursty, as indicated by smaller burst indices (median 1.41 for narrow spiking, median 3.58 for broad spiking, $p < 0.0001$, Mann-Whitney U-test). This is consistent with previous studies that have examined similar ratio metrics based on the size of early peaks in either the ISI distribution (Constantinidis and Goldman-Rakic, 2002) or early peaks in the auto-correlation function (Bartho et. al. 2004). Among the narrow spiking neurons, the majority (N=35/43, 81%) clustered around a relatively low burst index, but a small subset (N=8/43, 19%), indicated by the red dashed box had larger indices. This small subset may correspond to chattering neurons, as indicated in the Discussion section of the main text.

References

Bair,W., and O'Keefe, L.P. (1998). The influence of fixational eye movements on the response of neurons in area MT of the macaque. *Vis. Neurosci.* 15, 779-86.

Bartho P, Hirase M, Monoconduit L, Zugaro M, Harris KD, Buzsaki G (2004). Characterization of neocortical principle cells and interneurons by network interactions and extracellular features. *J. Neurophysiol*. 92:600-8.

Berry MJ 2nd and Meister M (1998). Refractoriness and neural precision. *J. Neurosci*. 18:2200-11.

Constantinidis C and Goldman-Rakic PS (2002). Correlated discharges among putative pyramidal neurons and interneurons in the primate prefrontal cortex. *J. Neurophysiol.* 88:3487-97.

Gur M, Beylin A, and Snodderly DM (1997). Response variability of neurons in primary visual cortex (V1) of alert monkeys. *J. Neurosci*. 17:2914-20.

Gur M, Beylin A, and Snodderly DM (1999). Physiological properties of macaque V1 neurons are correlated with extracellular spike amplitude, duration, and polarity. *J. Neurophysiol.* 82: 1451-1464.

Hartigan and Hartigan PM (1985). The dip test of unimodality. *Annals of Statistics.* 13:70-84.

Leopold DA and Logothetis NK (1998). Microsaccades differentially modulate neural activity in the striate and extrastriate visual cortex. *Exp. Br. Res.* 123:341-5.

Martinez-Conde S, Macknik SL, and Hubel DH (2000). Microsaccadic eye movements and firing of single cells in the striate cortex of macaque monkeys. *Nature Neurosci.* 3: 251-258.

McAdams CJ and Maunsell JH (1999a) Effects of attention on orientation tuning functions of single neurons in macaque cortical area V4. *J. Neurosci.* 19, 431-441.

McAdams CJ and Maunsell JH (1999b) Effects of attention on the reliability of individual neurons in monkey visual cortex. *Neuron.* 23:765-73.

Zuber BL, Stark L, and Cook G (1965). Microsaccades and the velocity-amplitude relationship for saccadic eye movements. *Science* 150:1459-1460.